

Chemical Profile of Drug Infused Papers Seized in Rio de Janeiro (Brazil) Prisons During the COVID-19 Lockdown

Adriana S. de Oliveira,^a Ananda S. Antonio,^{ib}*^b Cecília A. Bhering,^b Gleicielle T. Wurzler,^b Fernando G. de Almeida,^a Diego R. Carvalhosa,^{ac} Marco Antônio M. de Oliveira,^{ad} Francisco R. de Aquino Neto^b and Gabriela V. Costa^b

^aSecretaria de Estado de Polícia Civil (SEPOL), Instituto de Criminalística Carlos Éboli (ICCE), 20060-050 Rio de Janeiro-RJ, Brazil

^bLaboratório de Apoio ao Desenvolvimento Tecnológico (LADETEC), Núcleo de Análises Forenses (NAF), Instituto de Química, Universidade Federal do Rio de Janeiro, 21941-909 Rio de Janeiro-RJ, Brazil

^cSecretaria de Estado de Polícia Civil (SEPOL), Instituto Médico Legal Afrânio Peixoto (IMLAP), 20220-310 Rio de Janeiro-RJ, Brazil

^dDepartamento de Química Analítica (GQA), Instituto de Química, Universidade Federal Fluminense, 24020-141 Niterói-RJ, Brazil

Coronavirus disease (COVID-19) pandemic affected several business segments due to the lockdown period, including the illicit drug market. As Brazil usually imports new psychoactive substances (NPS), it was expected that their traffic would change during the pandemic. This study aimed to characterize NPS infused in pieces of paper seized inside prisons in the State of Rio de Janeiro (RJ), Brazil, during the COVID-19 pandemic by gas chromatography coupled with mass spectrometry, attenuated total reflectance-Fourier transform infrared spectroscopy, and high-resolution mass spectrometry. All samples were identified as synthetic cannabinoid receptor agonists, with indole-indazole structures. It was the first record of methyl (2*S*)-3,3-dimethyl-2-(1-(pent-4-en-1-yl)-1*H*-indazole-3-carboxamido) butanoate (MDMB-4en-PINACA), *N*-[(2*S*)-1-amino-3,3-dimethyl-1-oxobutan-2-yl]-1-butylindazole-3-carboxamide (ADB-BUTINACA), and *N*-(1-adamantyl)-1-(4-fluorobutyl)indazole-3-carboxamide (4F-ABUTINACA) in RJ, demonstrating that new NPS still arrived despite the lockdown. The integration of the data obtained via this study enabled the unequivocal identification of NPS even in the absence of standard reference materials, which is a common drawback faced by forensic laboratories in the analysis of NPS.

Keywords: synthetic cannabinoid receptor agonists, synthetic cannabinoids, blotter paper, GC-MS, orbitrap-HRMS

Introduction

The coronavirus disease (COVID-19) virus spread was a watershed in the recent society history. The severe clinical consequences of this virus induce several politics in an attempt to contain its outbreak. One of the effects politics used was the lockdown, restraining people's circulation, and closing commercial routes.¹ After more than three years, the World Health Organization (WHO) declared the end of the pandemic outbreak of COVID-19.² Despite it is officially over, the consequences of it remain, and it is unlike that

society will return to be like it was before COVID-19. Several business segments were deeply impacted and induced to be reinvented to maintain their profits due to the lockdown period.^{1,3,4} Even the illicit drug market had reinvented itself during COVID-19 pandemic.⁵

The mobility restriction imposed by COVID-19 lockdown and the partial close of international borders had a deep and heterogeneous impact in the illicit drug market depending on the country.⁵ In general, as most of the trafficking relies on the legal trade of commodities to camouflage from authorities, a shortage of drug supply was observed in several countries.⁶ The shortening of the supply chain of illicit drugs also induced changes in the price, users' profile, traffic routes, chemical profile, and availability of

*e-mail: ananda.antonio@gmail.com

Editor handled this article: Eduardo Carasek



different types of drugs.⁷⁻⁹ For instance, drugs such as cocaine and opiates, which are produced in only a few locations around the world, had presented a reduction in availability. Meanwhile, synthetic drugs had changed their profile in each country, due to the shortening of certain precursors for its synthesis.^{5,6} During the COVID-19 lockdown period, it has been observed in several countries a significant increase in the seizure and consumption of synthetic drugs and new psychoactive substances (NPS), when compared to their historical growth pattern (which was observed from 1998 to 2000).¹⁰ In the case of synthetic drugs and NPS, the COVID-19 lockdown did not even inhibit the appearance of novel substances in the market.^{7,10,11}

The so-called NPS rose during COVID-19 as their production is not limited by geolocation and they can be produced by several distinct synthetic routes.⁶ The emergence of NPS was a strategy to circumvent international drug regulations. As these drugs have different chemical structures than the already known drugs, they can pass undetected in most screening tests, and still produce psychotropic effects in the user.¹² By August 2020, over 1,000 NPS had emerged on the global illicit drug market.¹³ Over the past 10 years, Brazil has reported the identification of 116 NPS, being the country with the largest seizures of these drugs among the South American, Central American, and Caribbean countries.^{13,14}

Since NPS are designed to mimic other drugs already trafficked, they can be of many types, such as synthetic cathinone, amphetamine-like, synthetic hallucinogens, and synthetic cannabinoid receptor agonists (SCRAs).^{15,16} Cannabis and its by-products are the most trafficked drugs,¹⁰ and therefore, most of the NPS are also SCRAs.^{15,16}

The SCRAs are typically produced and transported as bulk powders and then dissolved in solvents such as acetone or methanol. Afterward, they are typically sprayed onto paper or herbal preparations to minimize the risk of detection and facilitate access to the end-user.^{15,17} For this reason, they can be easily hidden or smuggled. In addition to their lower prices (in comparison to other NPS available),¹⁸ it is difficult to identify/detect novel drugs or still unknown metabolites in urine samples.^{19,20} Due to these characteristics, SCRAs are mainly consumed by vulnerable social groups, such as prisoners. For instance, their abuse rate in the general population of England and Wales ranges from 3 to 11%, whereas it has been estimated to range from 60 to 90% among prisoners.^{18,21} The use of SCRAs was first detected in English and Welsh prisons in 2010-2011.²¹ In 2017, 22 European countries reported that SCRAs were the NPS group most often used in prison.²¹

Between 2016 and 2020, several seizures of paper containing SCRAs were carried out in Brazilian prisons

(São Paulo State).¹⁴ The only reported seizure of SCRAs in Rio de Janeiro (RJ) occurred in 2016 in a street operation. On this occasion, the substance FUB-AKB-48 (synthetic adamantyl cannabinoid) was detected in infused drug blotter paper.²² Other Brazilian states, such as Minas Gerais²³ and Santa Catarina,²⁴ have detected the presence of SCRAs in LSD-like (lysergic acid diethylamide) blotter paper and herbal preparations, in 2015 and 2017, respectively. In 2021, a significant increase in the identification of SCRAs in papers was reported in the Brazil Federal District and Minas Gerais state, with the substances MDMB-4en-PINACA (methyl (2*S*)-3,3-dimethyl-2-(1-(pent-4-en-1-yl)-1*H*-indazole-3-carboxamido) butanoate), 5F-MDMB-PICA (methyl 2-(1-(5-fluoropentyl)-1*H*-indole-3-carboxamido)-3,3-dimethylbutanoate), 5-chloro-MDMB-PICA (methyl (2*S*)-2-[[1-(5-chloropentyl)indole-3-carbonyl]amino]-3,3-dimethylbutanoate), 5F-PB-22 (quinolin-8-yl 1-(5-fluoropentyl)indole-3-carboxylate), CBL-2201 (naphthalen-1-yl 1-(5-fluoropentyl)indole-3-carboxylate), and ADB-BUTINACA (*N*-[(2*S*)-1-amino-3,3-dimethyl-1-oxobutan-2-yl]-1-butylandazole-3-carboxamide) being the most common.²³ Prior to the pandemic, there were no reports of SCRAs being seized inside any prison in RJ. However, the last report on drug seizures in the State of Rio de Janeiro was published in 2016 by the Public Security Institute, and since then there has been no official publication regarding the drugs seized in the region.²⁵

Monitoring drug seizures and availability is an important tool for the creation of public health and security strategies to mitigate drug traffic and its impact on society. Since many countries have been reporting changes in the illicit drug market and consumption pattern, it is crucial to keep surveillance in order to evolve police intelligence even in the face of the possible new strategies adopted by drug traffic. Therefore, this study carried out the chemical characterization of NPS-infused paper samples seized in RJ prisons during the COVID-19 pandemic. Identification of NPS within Brazilian prisons during the pandemic lockdown period can give insight into the drug trafficking trend that can occur in South America, as Brazil is the country with the largest occurrence of this type of drug and comprises several exportation routes of drugs of abuse.²⁶

Experimental

Sample collection and extraction

The evaluated samples were provided by the Civil Police of the State of Rio de Janeiro (PCERJ). Each sample was correlated with a specific seizure performed within RJ prison facilities (Table 1). During the COVID-19

lockdown period (from March 2020 to September 2021), the PCERJ performed eleven seizures, collecting a total of 1,726 pieces of paper. From each seizure, 15 pieces of paper were taken randomly to compose each of the evaluated samples (Table 1), with exception of sample B, which was provided in full (seven pieces). The number of pieces of paper provided was chosen following the internal PCERJ operational procedures for qualitative analysis and counter-evidence preservation, which establish a fixed number of samples *per* seizure as 15 units. Such sampling strategy is corroborated by the United Nations Office on Drugs and Crime (UNODC)²⁷ as an acceptable practice in illicit drug analysis as each seizure can have a specific characteristic that could make statistical-based sampling unpractical for most of police forces.

From each group of 15 pieces of paper, five were taken to perform the extraction required for gas chromatography coupled to mass spectrometry (GC-MS) and high resolution mass spectrometry (HRMS) by direct infusion analysis. Each of these subsets was extracted with 1.0 mL of methanol 99.9% (Tedia LTDA, São Paulo, SP, Brazil), homogenized via vortexing (LP vortex mixer, Thermo Scientific, Inc., Waltham, MA, USA) for 10 s, and centrifuged at 2,000 rpm for 4 min at room temperature (Centrifuge Excelsa Baby II 206-R, FANEM, São Paulo, SP, Brazil). The ten remaining pieces of paper were extracted via the same method and evaporated until dry, and the obtained crystals were loaded directly onto an attenuated total reflection Fourier transformed infrared (ATR-FTIR) equipment for analysis.

For sample B, which was composed by seven pieces of paper (Table 1), only one extract was prepared, using all

seven pieces. In this case, the entire extract was evaporated and crystallized after the GC-MS and Orbitrap-HRMS analysis, for the ATR-FTIR procedure.

GC-MS analyses

The GC-MS analyses were performed on a Thermo Scientific Trace 1310 gas chromatograph coupled to an ISQ 7000 single quadrupole mass spectrometer (Thermo Fisher Scientific Inc., Waltham, MA, USA). Chromatographic separation was performed using a HP-5MS capillary column (30 m × 0.25 mm i.d., 0.25 μm stationary phase thickness) (Agilent, Santa Clara, CA, USA) with helium (99.999%) (White Martins, Rio de Janeiro, RJ, Brazil) as the carrier gas at a flow rate of 1.0 mL min⁻¹. The sample solution (1.0 μL) was injected in split mode (30:1) at 250 °C using a TriPlus RSH autosampler (Thermo Scientific, Waltham, MA, USA). The temperature program was adapted from Meira *et al.*,²² as follow: isotherm at 50 °C for 1 min; increase to 200 °C at a rate of 30 °C min⁻¹; increase to 300 °C at a rate of 50 °C min⁻¹; isotherm at 300 °C for 1 min; increase to 330 °C at a rate of 80 °C min⁻¹; 13.3 min of total run time. The GC-MS interface temperature was 300 °C, and the solvent delay was set to 4 min. Electron ionization mass spectrometry was performed at 70 eV, and the mass spectra were acquired in full-scan mode. The full-scan acquisition range was *m/z* 40-450. All compounds were identified using commercial libraries (National Institute of Standards and Technology6-NIST Mass Spectral Library version 2.0) and the Scientific Working Group for the Analysis of Seized Drugs (SWGDRUG) 3.9 library.

Table 1. Identification of sample sets and number of pieces of papers

Sample ID	Date	Prison location (City)	Seizure size ^a	Sample size ^a for GC-MS and Orbitrap-HRMS analysis	Sample size ^a for ATR-FTIR analysis	Area / mm ²
A	11/11/2020	Magé	80	5	10	3.9
B	10/18/2020	Magé	7	7 ^b	7 ^b	16
C	09/04/2020	São Gonçalo	500	5	10	16
D	09/04/2020	São Gonçalo	500	5	10	16
E	12/20/2020	Magé	265	5	10	4
F	04/08/2021	São Gonçalo	66	5	10	15
G	04/08/2021	São Gonçalo	106	5	10	25
H	04/29/2021	Rio de Janeiro	22	5	10	16
I	08/13/2021	Rio de Janeiro	76	5	10	16
J	09/08/2021	Rio de Janeiro	62	5	10	16
K	04/23/2021	São Gonçalo	42	5	10	700
Total of seized papers			1,726			

^aNumber of pieces of paper; ^bThe same pieces of paper were used for all analysis; sample ID: sample identification code; GC-MS: gas chromatography coupled to mass spectrometry; Orbitrap-HRMS: high resolution mass spectrometry with an Orbitrap mass analyzer; ATR-FTIR: attenuated total reflection Fourier transformed infrared.

HRMS analysis

The analysis was performed on a high-resolution Q-Extractive Plus Orbitrap mass spectrometer (Orbitrap-HRMS) (Thermo Fisher Scientific, Bremen, Germany) equipped with an electrospray ionization (ESI) source to determine the exact masses of the various SCRA detected and their fragments. For this analysis, an aliquot (1.5 μL) of the extract was diluted to 1:1,000 with methanol 99.9% (Tedia LTDA, São Paulo, SP, Brazil), and 50 μL of 99% formic acid (Sigma-Aldrich, São Paulo, SP, Brazil) was added to promote the ionization of the analytes. Samples were injected at a flow rate of 10 $\mu\text{L min}^{-1}$. The spray voltage was set to 3.6 kV in positive ionization mode, or ESI(+); the capillary temperature was 380 $^{\circ}\text{C}$, and the S-lens radio frequency (RF) level was set to 60 (arbitrary units). The nitrogen sheath was set to 10 (arbitrary units). The dynamic range of ion acquisition in the Orbitrap analyzer was m/z 50-700. To ensure mass accuracy within 6 ppm, external calibration was performed for ESI(+) mode using a solution containing caffeine, MRFA (Met-Arg-Phe-Ala Acetate Salt), and Ultramark[®] 1621 (Thermo Scientific Solutions, Waltham, MA, USA). Analyses were performed with a resolution power of 140,000 FWHM (full width at half maximum) at m/z 200. The collision energy between 10 and 20 eV was used for the selective fragmentation of the analytes in MS/MS analyses. The mass spectra were acquired and processed using XCalibur software, version 2.2 (Thermo Fisher Scientific, Bremen, Germany).

ATR-FTIR analysis

The infrared (IR) spectrum of each sample was obtained using a Spectrum Two Fourier-transform infrared PerkinElmer Spectrometer with a diamond to achieve attenuated total reflection (PerkinElmer, Waltham, MA, USA). Each spectrum was acquired in a single mode with a resolution of 4 cm^{-1} , in the region ranging from 4000 to 550 cm^{-1} , and recorded with an average of four scans. The ATR-FTIR spectra obtained were compared with those from the literature (Supplementary Information (SI) section) or the equipment library (SWGDRUG IR Library, version 2.1, August 27, 2019).

Results and Discussion

All seized samples consisted of square and triangular pieces of paper with yellowish or orange colors (Figure 1), which ranged in size from 3.9 to 700 mm^2 (Table 1). A previous study¹⁷ included infused drug papers with a size of nearly 1 cm^2 . The variability observed in RJ prisons

emphasizes the versatility of this type of drug when manipulated by prisoners. For instance, by cutting a larger or smaller piece of the infused drug paper, they can adapt the paper to being hidden or smuggled more easily and regulate its dosage and administration form, as smaller pieces can enable contact through the eye or sublingually.¹⁷

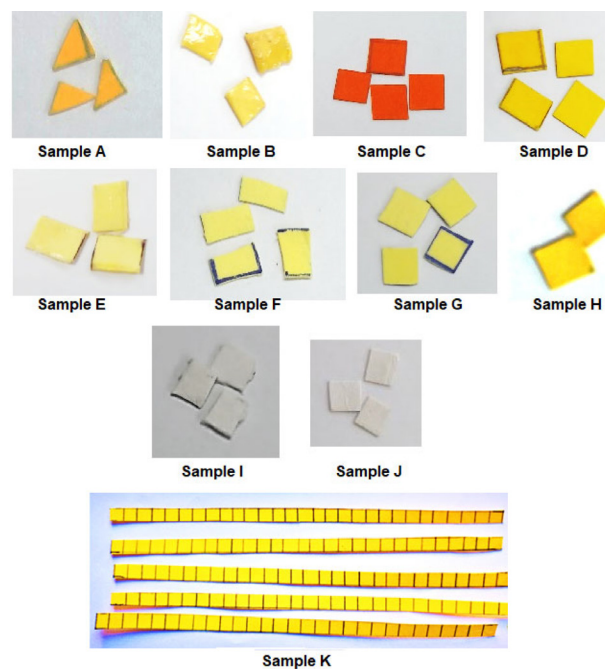


Figure 1. Samples physical appearance.

Among the eleven sets of samples (Table 1), four SCRA were identified (Table 2 and Figure 2). No other illicit drugs or substances, e.g., adulterants, were detected in any of these samples. All the identifications were performed by combining the information gathered by three types of analyses: GC-MS, direct infusion HRMS in full scan and MS/MS modes, and ATR-FTIR. In order to be considered a positive identification, the putative suggestion had to present on GC-MS analysis a similarity match higher than 900 (which corresponds to a similarity higher than 90%, considering the values of the m/z signals and their relative intensities) with SWGDRUG (Scientific Working Group for the Analysis of Seized Drugs), HRMS analysis of the precursor ion and fragments with less than ± 5 ppm of error, and IR spectrum compatible to those present in the SWGDRUG IR Library and the literature (SI section). It is worth mentioning that identification without any reference standard is a practice that can be adopted by forensic laboratories due to the constantly increasing number and diversification of NPS in the illicit market, which makes it difficult for most laboratories to keep pace with the acquisition of all reference standards, without knowing if such substances will ever be encountered in their location

or will keep being found with constancy.^{28,29} Surely, such practice must be performed only in the presence of high-performance methods, such as high-resolution mass spectrometry and nuclear magnetic resonance, and with the aid of updated libraries.²⁸⁻³⁰ In the case of this study, we used three distinct methods, including the HRMS, and an international library of chemical data for abuse drugs (SWGDRUG).

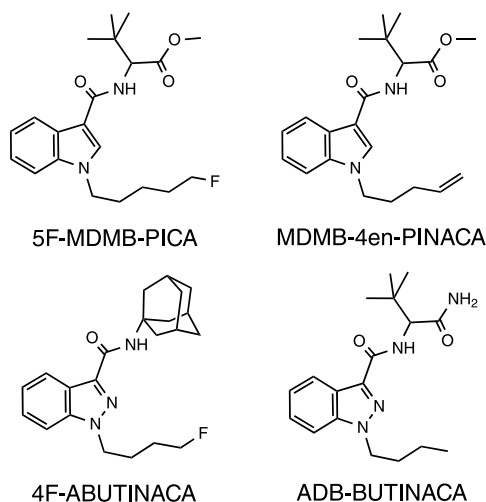


Figure 2. Chemical structure of the synthetic cannabinoid receptor agonists detected in the seized samples.

Characterization of the SCRAs detected

5F-MDMB-PICA

The analyses of samples containing 5F-MDMB-PICA by GC-MS were characterized by a chromatographic signal at the retention time (t_R) of 10.4 min (Figure S1a, SI section), with a mass spectrum containing the m/z signals 144, 232, 260, 288, 320, and 376 (Figure S2a, SI section). The identification of this chromatographic signal as 5F-MDMB-PICA was initially based on the strong similarity (match > 900) that its fragmentation

spectrum (Figure S2a) presented with the data available in the SWGDRUG spectrum library for 5F-MDMB-PICA. Mogler *et al.*³³ and Kleis *et al.*³⁴ proposed that the fragmentation pattern of 5F-MDMB-PICA is characterized by an acylium-indol-fluoroalkyl ion at m/z 232 ($C_{14}H_{15}FNO^+$) as its base peak, and an acylium-indole ion (m/z 144, $[C_9H_5NO^+]$) corresponding to the presence of an indole-carboxy moiety. In the fragmentation spectrum, the ion m/z 320 (corresponding to the loss of a *tert*-butyl group) may be formed based on a McLafferty-type rearrangement.³³

The infrared spectrum of 5F-MDMB-PICA (Figure S3a, SI section) showed a sharp band at 3437 cm^{-1} , representing N–H stretching of the amide group; C–H stretching vibrations of the alkyl occurred in the range $3000\text{--}2800\text{ cm}^{-1}$; and a weak aromatic C–H stretching band was present at 3104 cm^{-1} . Ester and amide carbonyl group modes appeared at 1729 and 1633 cm^{-1} , respectively. Another identified group was the alkyl fluoride attached to the nitrogen in indole, by the presence of a peak at 1033 cm^{-1} , with low intensity. The peak frequencies identified for indole were: 1530 and 751 cm^{-1} , which belong to the vibrations C=C symmetric stretch and C–C stretching, respectively. GC-MS and ATR-FTIR were important analytical techniques for their detection due to the lack of colorimetric tests for screening these drugs.

Afterward, high-resolution mass spectrometry played a pivotal role to confirm the chemical structure based on its fragmentation pattern. The full scan and MS/MS analyses (Figure S4a, SI section) allowed the determination of the exact mass of 5F-MDMB-PICA precursor and product ion (Table 3). During full scan analysis, the sodium adduct $[M + Na]^+$ was observed at m/z 399.20557. In MS/MS analysis the fragment $C_{14}H_{15}FNO^+$ observed is formed due to the cleavage of the amide bond of 5-MDMB-PICA. Due to the lack of reference standards for this NPS, HRMS was an important analytical tool for its identification.

Table 2. List of the four synthetic cannabinoids found in the samples, their chemical structures, nomenclature, and number of seizures *per year* in the State of Rio de Janeiro (Brazil) prisons over the period from 2020 to 2021

Compound	IUPAC name	LogP	Detected in samples	Number of seizures	
				2020	2021
5F-MDMB-PICA	methyl (2 <i>S</i>)-2-[[1-(5-fluoropentyl)indole-3-carbonyl]amino]-3,3-dimethylbutanoate	4.3 ^a	A, B, C and D	4	0
MDMB-4en-PINACA	methyl (2 <i>S</i>)-3,3-dimethyl-2-[(1-pent-4-enylindazole-3-carbonyl)amino]butanoate	4.3 ^a	E, F and G	1	2
ADB-BUTINACA	<i>N</i> -[(2 <i>S</i>)-1-amino-3,3-dimethyl-1-oxobutan-2-yl]-1-butylindazole-3-carboxamide	3.1 ^a	H, I and J	–	3
4F-ABUTINACA	<i>N</i> -(1-adamantyl)-1-(4-fluorobutyl)indazole-3-carboxamide	4.2 ³¹	K	–	1

^aXLogP3-AA value calculated by Cheng *et al.*³² computational method. IUPAC: International Union of Pure and Applied Chemistry; logP: partition coefficient between octanol and water.

Table 3. Molecular formulas, collision energies, experimental accurate masses of product ions, and error values of the synthetic cannabinoids analyzed by ESI(+)-Orbitrap-HRMS

Compound	[M + H] ⁺	Theoretical (<i>m/z</i>)	Exp. (<i>m/z</i>)	Error / ppm	CE / eV
5F-MDMB-PICA	C ₂₁ H ₃₀ N ₂ O ₃ F	377.22350	377.22324	-0.69	10
	C ₁₄ H ₁₅ N ₁ O ₁ F	232.11322	232.11314	-4.61	
MDMB-4en-PINACA	C ₂₀ H ₂₈ N ₃ O ₃	358.21252	358.21240	-0.32	17
	C ₁₈ H ₂₄ N ₃ O	298.19194	298.19116	-2.61	
	C ₁₃ H ₁₃ N ₂ O ₂	231.11335	231.11273	-2.68	
	C ₁₃ H ₁₃ N ₂ O	213.10279	213.10218	-2.86	
ADB-BUTINACA	C ₁₈ H ₂₇ N ₄ O ₂	331.21285	331.21284	-0.03	10
	C ₁₈ H ₂₄ N ₃ O ₂	314.18630	314.18589	-1.30	
	C ₁₇ H ₂₄ N ₃ O ₁	286.19139	286.19109	-1.15	
	C ₁₂ H ₁₃ N ₂ O ₁	201.10224	201.10173	-2.53	
4F-ABUTINACA	C ₂₂ H ₂₉ FN ₃ O	370.22892	370.22821	-1.91	20
	C ₁₀ H ₁₅	135.11683	135.11679	-0.30	

[M + H]⁺: molecular formula of the compound on its protonated form. Exp: experimental *m/z*; CE: collision energy.

MDMB-4en-PINACA

The GC-MS analysis of samples containing MDMB-4en-PINACA presented a chromatographic signal at *t_R* of 9.6 min and a mass spectrum with the *m/z* signals 131, 145, 213, 269, 301, and 357 (Figures S1b and S2b, SI section). This mass spectrum pattern presents a strong match (match > 900) with the SWGDRUG spectrum library database for PINACA-SC. A common structural element of PINACA-SC is an indazole ring with a pentyl chain and a carboxamide link.³⁴ The representative mass spectrum of MDMB-4en-PINACA (observed in all samples containing it) showed an acylium-indazole-alkyl ion at *m/z* 213 (C₁₃H₁₃N₂O⁺) as the base peak, similar to the main ion in the EI-MS spectrum of other SC with carboxyindazole cores.^{34,35} The presence of an acylium-indazole ion (*m/z* 145, [C₈H₅N₂O⁺]) and methyldiene-indazolium ion (*m/z* 131, [C₈H₅N₂O⁺]) in the mass spectrum, confirmed the presence of indazole-carboxy moiety, as reported by Dybowski *et al.*³⁶

The *m/z* 301 (C₁₆H₁₉N₃O₃⁺) fragment ion was formed by the McLafferty rearrangement of the *m/z* 357 (molecular ion).^{35,37} The molecular ion [M⁺] with *m/z* 357 (Figure S3b, SI section), observed in the mass spectrum obtained by GC-MS and the determination of its exact by Orbitrap-HRMS (Table 3), corroborated its identification. In the full scan analysis by HRMS, sodium adduct [M + Na]⁺ was observed at *m/z* 380.19455 (Figure S4b). The MS/MS analysis generated the expected product ions (Table 3). The results were consistent with Dybowski *et al.*,³⁶ who studied characteristic product ions with the influence of the applied fragmentation energy (CE) during MS/MS analysis with direct injection. The infrared spectrum of MDMB-4en-PINACA (Figure S3b) presented a band

at 3414 cm⁻¹, representing N–H stretching of the amide group; weak aromatic and alkene C–H stretching bands were present in the region from 3100 to 3000 cm⁻¹.³⁵ Ester and amide carbonyl group modes appeared at 1728 and 1666 cm⁻¹, respectively. The out-of-plane bending modes of alkene C–H bonds appeared at 925 cm⁻¹, and the contribution of in-plane vinyl bending was observed at 1215 and 1328 cm⁻¹. The main peak for the C=N bond in the indazole group was observed at 1520 cm⁻¹, and *tert*-butyl C–H appeared at 1029 cm⁻¹.

ADB-BUTINACA

Samples containing the ADB-BUTINACA compound presented an intense chromatographic peak at *t_R* = 9.9 min in GC-MS analysis (Figure S1c, SI section) and a mass spectrum with the *m/z* signals 131, 145, 201, 257, and 286 (Figure S2c, SI section). The mass spectrum presented an acylium-indazole-alkyl ion at *m/z* 201 (C₁₂H₁₃N₂O⁺) as the base peak, an acylium-indazole ion (*m/z* 145, [C₈H₅N₂O⁺]), and a methyldiene-indazolium ion (*m/z* 131, [C₈H₅N₂O⁺]). The *m/z* 286 (C₁₇H₂₄N₃O⁺) fragment ion was formed with the loss of the NH₂C=O group. Comparing the GC-MS and HRMS analyses of ADB-BUTINACA, the molecular ion was only observed in the HRMS analysis ([M + H]⁺ = 331.21284, error = -0.03 ppm), which allowed the determination of the exact mass and confirmed its identification (Table 3). In the full scan analysis, sodium adduct [M + Na]⁺ was observed at *m/z* 353.19479 (Figure S4c, SI section). The MS/MS analyses allowed the determination of the product ions with *m/z* 286.19109 and 201.10173, corresponding to the fragments (C₁₇H₂₄N₃O⁺) and (C₁₂H₁₃N₂O⁺), respectively. The product ion *m/z* 314.18589 was generated by the neutral

loss of NH_3 from m/z 331.21284.³⁷ The infrared spectrum of ADB-BUTINACA (Figure S3c, SI section) showed a band at 3376 cm^{-1} , representing N–H stretching of the amide group; and weak aromatic and alkene C–H stretching bands were present in the region from 3100 to 3000 cm^{-1} .³⁵ The amide carbonyl group band appeared at 1691 cm^{-1} . The main peak for the C=N bond in the indazole group was observed at 1528 cm^{-1} , and *tert*-butyl C–H appeared at 1032 cm^{-1} . The main peaks identified for this compound were shown at 1648 cm^{-1} , corresponding to the secondary amide group (C=O stretch), and a second band for the same functional group (C–N–C) was observed at 1491 cm^{-1} .

4F-ABUTINACA

The samples containing 4F-ABUTINACA were characterized by an intense chromatographic peak at the t_R 11.7 min (Figure S1d, SI section) and a mass spectrum with the m/z signals 131, 145, 219, 284, 294, 324, 341, and 369 (Figure S2d, SI section), in accordance with the SWGDRUG (version 3.9) mass spectra library (match > 900).³⁸ Adamantylindazole carboxamide showed a molecular ion $[\text{M}^+]$ with m/z 369 and a base peak at m/z 219, corresponding to the fragmentation of the C–N amide bond (Figure S2d, SI section). The fragment ion at m/z 219 ($\text{C}_{12}\text{H}_{12}\text{FN}_2\text{O}^+$) was considered to have arisen from the acylium ion ($\text{R}-\text{C}\equiv\text{O}^+$), and the fragment at m/z 150 to have arisen from the ion ($[\text{adamantylamine}-\text{H}]^+$). There were fragment ions at m/z 341 ($[\text{M} - 28]^+$), m/z 294 (loss of the alkyl group), and m/z 145 (an acylium-indazole ion $[\text{C}_8\text{H}_3\text{N}_2\text{O}^+]$), as observed by Asada *et al.*³⁹ The HRMS analysis confirmed 4F-ABUTINACA identification through MS/MS pattern, with the detection of the precursor ion $[\text{C}_{22}\text{H}_{28}\text{ON}_3\text{F} + \text{H}]^+$ and its fragment ion $[\text{C}_{10}\text{H}_{15}]^+$ originated from the adamantyl ring. The infrared spectrum from samples containing 4F-ABINACA (Figure S3d, SI section) showed the functional groups of SC as amide carbonyl stretching conjugated with an indazole group, with a characteristic absorption at 1662 cm^{-1} .

Forensic implications

The use of depressant-type drugs was more popular with prisoners, as they promote relaxation, have discreet effects on the user, and help ease boredom.¹⁸ However, previous studies²² with blotter papers seized on the streets of the State of Rio de Janeiro (RJ) demonstrate that the chemical profile of drug-infused papers seized in the state is mainly characterized by the occurrence of phenethylamines, a stimulant-drug type. The results indicate a drastic change in the chemical profile of drug-infused papers seized in RJ because none of the evaluated

samples contained phenethylamines. The discrepancy between our findings and those reported by Meira *et al.*²² suggests two hypotheses: (i) drugs smuggled into prison are distinct from those trafficked on the streets, and (ii) the chemical profile of drug-infused papers in Rio de Janeiro was drastically modified during the COVID-19 lockdown (from the end of 2019 until the first half of 2020). Before the COVID-19 pandemic, there were no reports of SCRA seizures neither within RJ prisons nor in the streets.

Chronologically, 5F-MDMB-PICA was the first SCRA seized within RJ prisons (Table 1). It was detected in samples A, B, C and D, which represented three seizures performed in 2020, with a total of 1,087 (62.98% of the total) papers seized (Table 2). In 2018, 5F-MDMB-PICA's first detection in Brazil occurred in a street seizure.¹² In the following years, the 5F-MDMB-PICA has been seized in street operations (in the form of infused papers), with a significant increase in 2021.^{12,23} Another large seizure of 5F-MDMB-PICA also occurred in prisons located in São Paulo (SP), a state located south of RJ, during the COVID-19 lockdown. In fact, 5F-MDMB-PICA was the major SCRA found in SP prisons from 2019 to 2020.¹⁴ Such a pattern indicates that this drug is preferred for smuggling in prison facilities due to the fact that the market is constantly changing in order to circumvent legislation and shortcomings in the availability and prices of raw materials and reagents for its synthesis.^{20,40} In 2016, 5F-MDMB-PICA was first detected in Europe and the US.⁴⁰ This SCRA was first detected in Brazil in 2018,²² but an increase in its trafficking began in 2019 and continued throughout the COVID-19 lockdown, being seized mainly inside prisons in SP, RJ, the Federal District, and Minas Gerais State.^{14,23} Such a pattern indicates that its presence in the country was not affected by the closure of borders prompted by the COVID-19 lockdown. Therefore, it is possible that it could have been provided via a local supplier, imported, or mailed directly to prison.^{14,41} This fact may suggest that, after the first seizure of 5F-MDMB-PICA in Brazil, in 2018,¹² local drug suppliers began to produce locally by 2019, as evidenced by the increase in seizures.

MDMB-4en-PINACA was detected in samples E, F, and G, which represented two seizures performed in 2020 and 2021, with a total of 437 pieces of paper (25.32% of the total) (Table 2). Although this SCRA has been available on the European drug market since 2017,³³ its arrival in Brazil occurred only in 2019, when it was first identified in São Paulo state prisons¹⁴ and in the state of Minas Gerais and Federal District.²³ Our data indicate that 5F-MDMB-PICA and MDMB-4en-PINACA were the major SCRA smuggled into RJ prisons (Table 2). The same

pattern was reported in SP prisons,¹⁴ indicating that both states may be part of the same trafficking route or supplier.

ADB-BUTINACA, or ADB-BINACA, is one of the most recent SCRA to emerge worldwide. It was reported in Europe (Sweden) in 2019.²¹ ADB-BUTINACA was identified only in seizures performed in 2021, being detected in the samples H, I, and J, which represent three distinct seizures containing a total of 160 pieces of paper (9.27% of the total seized) (Table 2). The first report of this SCRA in Brazil, however, occurred between 2016-2020, in an SP prison.¹⁴ The present data correspond to the first seizure of ADB-BUTINACA in RJ. After that, throughout 2021, several seizures of small quantities of ADB-BUTINACA in the form of drug-infused papers occurred in street police surveillance actions, most of them in SP.⁴² According to internal communications among Brazilian Civil Police from different states, ADB-BUTINACA's presence in Brazil has been increasing since the end of 2021, becoming one of the major SCRA's seized in prisons in the South and Southeast Regions of Brazil in 2022.

4F-ABUTINACA or 4F-ABINACA, was the least detected SCRA's (Table 2). However, this is the first time that this compound is detected in Brazil. 4F-ABUTINACA was detected in sample K, which represents a single seizure of 42 pieces of paper (2.43% of the total) that occurred in 2021. This drug was formally announced in the beginning of 2019.⁴³ 4F-ABUTINACA is classified as a fourth-generation SCRA's; thus, it is estimated to have more intense psychotropic effects and be more toxic than previous SCRA's.⁴³ Because its clinical effects remain unknown, along with efficient treatments for cases of intoxication, 4F-ABUTINACA has caught the attention of surveillance authorities. This compound was the only SCRA's that was identified as a mixture (with MDMB-4en-PINACA). Its appearance in a mixture suggests three hypotheses: (i) a shortage of MDMB-4en-PINACA, (ii) a market test regarding its acceptance, or (iii) contamination during the manufacturing process. If the second hypothesis is correct, it is expected that 4F-ABUTINACA will appear more frequently in the future.

Conclusions

Before the COVID-19 pandemic, Brazil was not characterized as a country with a significant SCRA's prevalence as compared to other countries, especially within the imprisoned population.¹⁴ The increase in the presence of SCRA's in Brazilian prisons indicates the modification of the illicit drug market. 5F-MDMB-PICA, MDMB-4en-PINACA, ADB-BUTINACA, and 4F-ABUTINACA were identified for the first time in Rio de Janeiro from infused papers

seized in RJ prisons during the COVID-19 pandemic. Among them, the 5F-MDMB-PICA compound was the most abundant SCRA, and 4F-ABUTINACA, was the newest SCRA identified in Brazilian prisons. It is worth mentioning that to date, there is no other record of 4F-ABUTINACA seizures in other South American countries, demonstrating the propagation of trafficking routes related to this fourth-generation SCRA's directly to Brazil. The popularization of SCRA's within prison facilities is an issue that has been occurring in Europe and the USA in the last decade and was not affected by the closure of international borders during the COVID-19 pandemic. Such a fact can aid the national and international early warning systems for law enforcement in the elucidation of smuggling and trafficking routes across countries. In addition, the data gathered can help the development of security systems and highlight targets for toxicological studies aiming at the health risk of newly detected SCRA's, such as the case of 4F-ABUTINACA.

Supplementary Information

Supplementary information is available free of charge at <http://jbc.sbj.org.br> as PDF file.

Acknowledgments

This study was financed in part by the Coordenação de Aperfeiçoamento de Pessoal de Nível Superior - Brazil (CAPES) - Finance Code 001. The authors are also grateful for the financial support provided by the Fundação de Amparo à Pesquisa do Estado do Rio de Janeiro (FAPERJ) and the Conselho Nacional de Desenvolvimento Científico e Tecnológico (CNPq).

Author Contributions

Adriana S. de Oliveira was responsible for conceptualization, methodology, writing original draft, investigation, formal analysis, data curation; Ananda da S. Antonio for writing original draft, formal analysis, visualization, data curation; Cecília A. Bhering for writing original draft, formal analysis, visualization, data curation; Gleicielle T. Wurzler for writing original draft, formal analysis, visualization, data curation; Fernando G. de Almeida for resources, writing (review and editing), supervision, funding acquisition; Diego R. Carvalhosa for conceptualization, resources, writing (review and editing), funding acquisition; Marco Antônio M. de Oliveira for resources, writing (review and editing), supervision, funding acquisition; Francisco R. de Aquino Neto for conceptualization, resources, writing review and editing; Gabriela Vanini for conceptualization, resources, project administration, supervision, writing review and editing.

References

1. Alabi, M. O.; Ngwenyama, O.; *Br. Food J.* **2023**, *125*, 167. [Crossref]
2. World Health Organization (WHO); *Coronavirus Disease (COVID-19) Pandemic*, <https://www.who.int/europe/emergencies/situations/covid-19>, accessed in November 2023.
3. Kaftan, V.; Kandalov, W.; Molodtsov, I.; Sherstobitova, A.; Strielkowski, W.; *Sustainability* **2023**, *15*, 2876. [Crossref]
4. Tan, X.; Ma, S.; Wang, X.; Feng, C.; Xiang, L.; *Front. Public Heal.* **2022**, *10*, 963620. [Crossref]
5. United Nations Office on Drugs (UNODC); *COVID-19 and Drugs: Impact Outlook*, https://www.unodc.org/res/wdr2021/field/WDR21_Booklet_5.pdf, accessed in November 2023.
6. United Nations Office on Drugs (UNODC); *COVID-19 is Changing the Route of Illicit Drug Flows, says UNODC report*, <https://www.unodc.org/unodc/en/press/releases/2020/May/covid-19-is-changing-the-route-of-illicit-drug-flows--says-unodc-report.html>, accessed in November 2023.
7. European Monitoring Centre for Drugs and Drug Addiction (EMCDDA); *Impact of COVID-19 on Drug Markets, Use, Harms and Drug Services in the Community and Prisons*, https://www.emcdda.europa.eu/publications/ad-hoc-publication/impact-covid-19-drug-markets-use-harms-and-drug-services-community-and-prisons_en, accessed in November 2023.
8. Otiashvili, D.; Mgebrishvili, T.; Beselia, A.; Vardanashvili, I.; Dumchev, K.; Kiriazova, T.; Kirtadze, I.; *Harm Reduct. J.* **2022**, *19*, 25. [Crossref]
9. Ziavrou, K. S.; *The Evolving Illicit Drug Market During the Covid-19 Pandemic*; <https://www.marshallcenter.org/en/publications/perspectives/evolving-illicit-drug-market-during-covid-19-pandemic-0>, accessed in November 2023.
10. United Nations Office and Drug and Crime (UNODC); *Booklet 2 - Global Overview of Drug Demand and Drug Supply*, https://www.unodc.org/unodc/en/data-and-analysis/wdr-2022_booklet-2.html, accessed in November 2023.
11. Catalani, V.; Arillotta, D.; Corkery, J. M.; Guirguis, A.; Vento, A.; Schifano, F.; *Front. Psychiatry* **2021**, *11*, 632405. [Crossref]
12. Instituto Nacional de Criminalística-Diretoria Técnico-Científica; Ministério da Justiça e Segurança Pública; *Relatório 2020-Drogas Sintéticas*, https://www.gov.br/pf/pt-br/acao-a-informacao/acoes-e-programas/relatorio-de-drogas-sinteticas-2020/relatorio_drogas_sinteticas_2020.pdf, accessed in November 2023.
13. United Nations Office and Drug and Crime (UNODC); *Global Synthetic Drugs Assessment 2020-Regional Overviews*, <https://www.unodc.org/unodc/en/scientists/2020-global-synthetic-drugs-assessment-regional-overviews.html>, accessed in November 2023.
14. Rodrigues, T. B.; Souza, M. P.; Barbosa, L. M.; Ponce, J. C.; Neves Jr., L. F. N.; Yonamine, M.; Costa, J. L.; *Forensic Toxicol.* **2022**, *40*, 119. [Crossref]
15. Shafi, A.; Berry, A. J.; Sumnall, H.; Wood, D. M.; Tracy, D. K.; *Ther. Adv. Psychopharmacol.* **2020**, *10*, 1. [Crossref]
16. Darke, S.; Banister, S.; Farrell, M.; Dufloy, J.; Lappin, J.; *Int. J. Drug Policy* **2021**, *98*, 103396. [Crossref]
17. Norman, C.; Walker, G.; McKirdy, B.; McDonald, C.; Fletcher, D.; Antonides, L. H.; Sutcliffe, O. B.; Nic Daéid, N.; McKenzie, C.; *Drug Test. Anal.* **2020**, *12*, 538. [Crossref]
18. Ralphs, R.; Williams, L.; Askew, R.; Norton, A.; *Int. J. Drug Policy* **2017**, *40*, 57. [Crossref]
19. Haschimi, B.; Mogler, L.; Halter, S.; Giorgetti, A.; Schwarze, B.; Westphal, F.; Fischmann, S.; Auwärter, V.; *Drug Test. Anal.* **2019**, *11*, 1377. [Crossref]
20. Norman, C.; Halter, S.; Haschimi, B.; Acreman, D.; Smith, J.; Krotulski, A. J.; Mohr, A. L. A.; Logan, B. K.; Nic Daéid, N.; Auwärter, V.; McKenzie, C.; *Drug Test. Anal.* **2021**, *13*, 841. [Crossref]
21. European Monitoring Centre for Drugs and Drug Addiction (EMCDDA); *New Psychoactive Substances Global Markets, Glocal Threats and the COVID-19 Pandemic: An Update from the EU Early Warning System*, <https://op.europa.eu/en/publication-detail/-/publication/7bd409b6-44cd-11eb-b59f-01aa75ed71a1>, accessed in November 2023.
22. Meira, V. L.; de Oliveira, A. S.; Cohen, L. S. A.; A. Bhering, C.; de Oliveira, K. M.; de Siqueira, D. S.; de Oliveira, M. A. M.; de Aquino Neto, F. R.; Vanini, G.; *Forensic Sci. Int.* **2021**, *318*, 110588. [Crossref]
23. Marinho, P. A.; Ricoy, C. R.; Arantes, L. C.; Gomes, E. B.; *Rev. CML* **2021**, *6*, 65. [Crossref]
24. Machado, Y.; Coelho Neto, J.; Lordeiro, R. A.; Silva, M. F.; Piccin, E.; *Forensic Toxicol.* **2019**, *37*, 265. [Crossref]
25. Instituto de Segurança Pública do Estado do Rio de Janeiro; *Panorama das Apreensões de Drogas no Rio de Janeiro 2010-2016*; Caldas, E. A. R. M., ed.; Instituto de Segurança Pública: Rio de Janeiro, 2016. [Link] accessed in November 2023
26. United Nations Office on Drugs and Crime (UNODC); *Drug Market Trends: Cocaine Amphetaminetype Stimulants*, https://www.unodc.org/res/wdr2021/field/WDR21_Booklet_4.pdf, accessed in November 2023.
27. United Nations Office on Drugs and Crime (UNODC); *Guidelines on Representative Drug Sampling*, https://www.unodc.org/documents/scientific/Drug_Sampling.pdf, accessed in November 2023.
28. Mesihää, S.; Rasanen, I.; Ojanperä, I.; *Forensic Sci. Int.* **2020**, *312*, 110304. [Crossref]
29. Gerostamoulos, D.; Elliott, S.; Walls, H. C.; Peters, F. T.; Lynch, M.; Drummer, O. H.; *J. Anal. Toxicol.* **2016**, *40*, 318. [Crossref]
30. de Campos, E. G.; Krotulski, A. J.; de Martinis, B. S.; Costa, J. L.; *Wires Forensic Sci.* **2022**, *4*, e1455. [Crossref]
31. Kim, S.; Thiessen, P. A.; Bolton, E. E.; Chen, J.; Fu, G.; Gindulyte, A.; Han, L.; He, J.; He, S.; Shoemaker, B. A.; Wang, J.; Yu, B.; Zhang, J.; Bryant, S. H.; *Nucleic Acids Res.* **2016**, *44*, D1202. [Crossref]

32. Cheng, T.; Zhao, Y.; Li, X.; Lin, F.; Xu, Y.; Zhang, X.; Li, Y.; Wang, R.; Lai, L.; *J. Chem. Inf. Model.* **2007**, *47*, 2140. [Crossref]
33. Mogler, L.; Franz, F.; Rentsch, D.; Angerer, V.; Weinfurter, G.; Longworth, M.; Banister, S. D.; Kassiou, M.; Moosmann, B.; Auwärter, V.; *Drug Test. Anal.* **2018**, *10*, 196. [Crossref]
34. Kleis, J.; Germerott, T.; Halter, S.; Héroux, V.; Roehrich, J.; Schwarz, C. S.; Hess, C.; *Forensic Sci. Int.* **2020**, *314*, 110410. [Crossref]
35. European Monitoring Centre for Drugs and Drug Addiction; *Report, EMCDDA Initial Report on the New Psychoactive Substance MDMA-4en-PINACA*, https://www.emcdda.europa.eu/publications/initial-reports/mdmb-4en-pinaca_en, accessed in November 2023.
36. Dybowski, M. P.; Holowinski, P.; Typek, R.; Dawidowicz, A. L.; *Forensic Toxicol.* **2021**, *39*, 481. [Crossref]
37. Sekuła, K.; Zuba, D.; Lorek, K.; *J. Am. Soc. Mass Spectrom.* **2018**, *29*, 1941. [Crossref]
38. Scientific Working Group for the Analysis of Seized Drugs; 2021, <https://www.swgdrug.org/ms.htm>, accessed in November 2023.
39. Asada, A.; Doi, T.; Tagami, T.; Takeda, A.; Sawabe, Y.; *Drug Test. Anal.* **2017**, *9*, 378. [Crossref]
40. United Nations Office and Drug and Crime (UNODC); *Synthetic Drugs in East and Southeast Asia Latest Developments and Challenges*, https://www.unodc.org/documents/scientific/ATS/2021_ESEA_Regional_Synthetic_Drugs_Report.pdf, accessed in November 2023.
41. World Health Organization (WHO); *Critical Review Report: 5F-MDMB-PICA*; WHO: Geneva, 2019. [Link] accessed in November 2023
42. Centre of Excellence for the Illicit Drug Supply Reduction; Narcotics Testing Centre; Brazilian Federal Police; *First Report of the Early Warning Subsystem on Drugs (EWS)*, <https://www.gov.br/mj/pt-br/assuntos/sua-protecao/politicas-sobre-drogas/subsistema-de-alerta-rapido-sobre-drogas-sar/1o-informe-do-sar-versao-ingles.pdf>, accessed in November 2023.
43. Malaca, S.; Tini, A.; Ronchi, F. U.; *Acta Biomed.* **2022**, *92*, e2021546. [Crossref]

Submitted: September 25, 2023

Published online: November 29, 2023